Nanotube Wires on Commensurate InAs Surfaces: Binding Energies, Band Alignments, and Bipolar Doping by the Surfaces

Yong-Hyun Kim, M. J. Heben, and S. B. Zhang
National Renewable Energy Laboratory, Golden, Colorado 80401, USA
(Received 3 February 2004; published 29 April 2004)

Using first-principles methods, we study the physicochemical properties such as the binding mechanism and band offset for single-wall zigzag nanotubes on InAs. While the tubes maintain their structural and electronic integrity, binding energies as large as 0.4 eV per site are obtained. Except for semiconducting tubes on the polar surfaces, an approximate universal band alignment is also obtained. The exception is due to large surface dipoles. In fact, polar (111) and $(\bar{1}\,\bar{1}\,\bar{1})$ surfaces have opposite dipoles that cause autodoping of a (14, 0) tube to the *n* and the *p* type, respectively, without actual dopant.

DOI: 10.1103/PhysRevLett.92.176102 PACS numbers: 68.43.Fg, 68.47.Fg, 72.20.Jv, 73.22.–f

Carbon nanotubes (CNTs) are truly remarkable because these simple nanostructures cover a whole range of electronic properties from being simple metals to semiconductors. Depending on the diameter and chirality of the wrapped-up honeycomb lattice, the band gap of a CNT can change quasicontinuously [1,2]. The recent realization of a CNT field-effect transistor (FET) [3] has caused much effort to be devoted to improving the CNT-FETs's properties by employing different gate materials, metal contacts, and geometries [4]. Very recently, Misewich *et al.* reported a miniature light-emitting device based on the CNT-FET architecture [5]. Despite the experimental progress, an atomistic understanding of the CNT junctions with semiconductors and/or oxides and the electronic properties of the interfaces is largely lacking.

From a fundamental point of view, it is not yet fully clear how the CNTs will behave as nanoelectronic materials. Will they behave as extended molecular chains, or will they conduct like an ordinary piece of metal or doped semiconductor, except for some measurable quantum size effects? When in contact with other materials, will the tube atoms be bound to, or alloyed with, the surface atoms? How much can one still treat the tube as a distinct entity with its own material properties and characteristics? How would such properties differ from those of isolated CNTs? Even though past experiments and theories have revealed consistently that an isolated single-wall CNT can have an appreciable band gap of up to 1.5 eV [1,2], it is not yet clear if the band gap here bears any resemblance to that of a bulk semiconductor under conditions suitable for device applications. Recently, it has been shown that the band structure (and band gap) of a CNT could be readily modified either by radial deformation or by external transverse electric field [6,7].

In this Letter, we use first-principles total energy methods to calculate the basic electronic properties of CNT/semiconductor interfaces. The approach yields information about band offsets, interfacial binding, Fermi-level position, and the charge transfer across the interface. We show that nanotubes bind to a binary semiconductor surface primarily through the coupling between cation dangling-bond orbitals and carbon π-bond orbitals. Indium arsenide is considered here for lattice commensuration with zigzag nanotubes $(n, 0)$, where $n = 6$, 10, 14, 17, 18. The calculated binding energies can be significant, e.g., 0.4 eV per binding site for a (6, 0) tube with nonpolar (110) and polar (111) surfaces. On the other hand, binding energy for an As-exposed $(\bar{1}\,\bar{1}\,\bar{1})$ surface is less than 0.2 eV per site, comparable to van der Waals–type dipole-dipole interactions. The band offsets for metallic tubes, and for semiconducting tubes on nonpolar surfaces, obey approximately a universal alignment rule, as can be expected from their unique relationships with the graphene Fermi level. On the other hand, semiconducting nanotubes on polar surfaces behave like giant molecules with their energy alignment strongly affected by surface dipole potentials. In the extreme cases, the nanotube valence band maximum (VBM) may be placed above the conduction band minimum (CBM) of InAs(111), or, conversely, the nanotube CBM may be placed below the VBM of InAs$(\bar{1}\,\bar{1}\,\bar{1})$. Thus, autodoping of nanotubes is possible by different surface orientations to both the *p* and the *n* type without any actual dopant.

Our calculations were performed based on the density functional theory [8] within the local density approximation (LDA). The Ceperley-Alder exchange-correlation energy functional was used [9]. We employed the ultrasoft pseudopotentials [10], as implanted in the VASP package [11]. The electron wave functions were expanded in the plane wave basis with a kinetic energy cutoff of 287 eV. We used a slab geometry for the surface calculations, which contains eight monolayers for the (110) surface and six double layers for the (111) and $(\bar{1}\,\bar{1}\,\bar{1})$ surfaces. The back surfaces are passivated with pseudohydrogen atoms. Three and five **k** points along the tube axis are used, respectively, for the Brillouin zone integration for the semiconducting and metallic tubes. It is well known

that LDA underestimates the band gap. This underestimation is, however, offset by the quantum confinement effect of the slabs. For example, the band gap for the (110) surface slab of 0.53 eV, by choice, comes close to the experimental value for bulk InAs of 0.43 eV at 0 K. We have optimized the atomic positions by minimizing the Hellmann-Feynman forces to less than 1 mRy/(a.u.) for all the atoms.

When placing a nanotube on a surface, it is natural to first consider how the lattices of the tube and the surface align. By surveying binary semiconductors, we found only a few cases where the lattices are commensurate, e.g., InAs and CdSe with zigzag nanotubes in the [110] directions (see Fig. 1). The carbon-to-carbon distance is 1.42 Å for graphite and 1.44 Å, on the average, for C_{60} [12]. Thus, the axial lattice parameter for zigzag nanotubes is between 4.260 and 4.320 Å. In comparison, the [110] lattice parameter for InAs is 4.284 Å. By choosing commensurate zigzag nanotubes on InAs, we can apply a periodic boundary condition in the calculations, with a minimum residual strain estimated to be less than 0.7%. This is in contrast to Ref. [13], where much larger artificial strain is unavoidable.

Among the zigzag tubes, (6, 0) is a metal due to its large surface curvature [14]; (10, 0), (14, 0), and (17, 0) are semiconductors with $E_g = 0.8$, 0.5, and 0.4 eV, respectively; (18, 0), on the other hand, is a semimetal with $E_g < 0.01$ eV. We consider both the nonpolar (110) surface and the polar (111) and $(\bar{1}\,\bar{1}\,\bar{1})$ surfaces terminated, respectively, by In and As vacancies. Usually, vacancy surfaces are expected to exist under cation-rich growth conditions [15].

Noninteracting nanotubes.—Figure 2 shows a band diagram for carbon nanotubes placed > 3.7 Å away from the nonpolar InAs(110) surface, far enough so that the tubes can be considered noninteracting with the surface. The band offsets are calculated by aligning the average potential in the bulk region of the slab with that of bulk InAs [17]. The dotted lines in Fig. 2 indicate the graphene Fermi level ($E_F^{\rm gr}$), which corresponds to the midgap energy position for semiconducting CNTs with diameter ≥ 6.5 Å [14]. It shows that $E_F^{\rm gr}$ for different tubes are aligned at 0.53 ± 0.08 eV above the VBM of InAs. The reason for the good alignment can be traced back to the zone folding method [12], which predicts accurate positions for tube band edge states from that of graphene. As is shown below, the significance of Fig. 2 is beyond the noninteracting case. From it, one can arrive at an approximate but "universal" estimate of the band diagram for any nanotube *interacting* with a nonpolar surface of InAs. If one replaces InAs by another III-V semiconductor whose band offset to InAs is known, e.g., InP in Fig. 2, it is also reasonable to expect that the rule applies. Thus, a (17, 0) tube is likely to have a type-II alignment with InAs(110), but a type-I alignment with InP(110). Later, we show that for metallic tubes on the polar surfaces, reasonably good $E_F^{\rm gr}$ alignment also exists. On the other hand, polar surface dipoles can have sizable effects on the semiconducting tubes, making Fig. 2 inapplicable.

Interacting nanotubes: I. Binding mechanism.—Relatively large binding energies are obtained for the (6, 0) tube on both (110) and (111) surfaces, i.e., 0.4 eV per [110] unit. In contrast, the binding energy for the $(6, 0)/(\bar{1}\,\bar{1}\,\bar{1})$ case is substantially smaller, only 0.1 eV per unit. In general, regardless of the diameter, nanotubes bind to the (110) and (111) surfaces more strongly than the $(\bar{1}\,\bar{1}\,\bar{1})$ surface, i.e., 0.3–0.4 per unit vs 0.1–0.2 eV per unit. A closer examination of the binding geometries and charge densities (not shown) reveals that the per-[110]-unit binding energy gains can be attributed to the formation of a weak bond between a surface In atom and a carbon-carbon pair on the tube. Table I thus

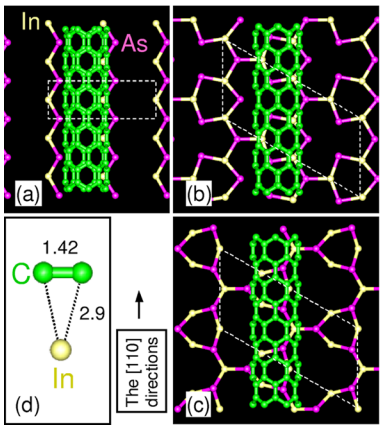

FIG. 1 (color online). Ball-and-stick models of a (6, 0) nanotube on (a) (110), (b) (111), and (c) $(\bar{1}\,\bar{1}\,\bar{1})$ surfaces of InAs. Only the topmost monolayer of each surface is shown. Dashed lines indicate supercells used in the calculation. (d) The binding configuration between a C-C pair on the nanotube and an In atom on the (110) and (111) surfaces. The bond lengths are given in Å.

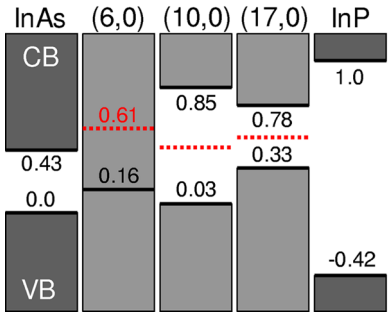

FIG. 2 (color online). Calculated band diagram for noninteracting (6, 0), (10, 0), and (17, 0) nanotubes on InAs(110). Dotted lines indicate $E_F^{\rm gr}$ (defined in the text), which line up to within ± 0.08 eV. For comparison, InP is also shown (its band alignment with InAs is taken from Ref. [16]).

TABLE I. Calculated binding energy between the $(n, 0)$ nanotubes and InAs (110), (111), and $(\bar{1}\,\bar{1}\,\bar{1})$ surfaces, in eV per binding site.

	(6, 0)	(10, 0)	(14, 0)	(17, 0)	(18, 0)
(110)	0.4	0.3	0.3	0.3	0.3
(111)	0.4	0.3	0.4		
$(\bar{1}\,\bar{1}\,\bar{1})$	0.1	0.2	0.2		

summarizes the binding energies in units of eV per binding site.

In both the (110) and (111) cases, the In atom and the carbon atoms in the C-C pair form an isosceles triangle, as shown in Fig. 1(d). The C-In distance of 2.9 Å is considerably smaller than the van der Waals distance of 3.6 Å, but larger than the covalent radius of 2.2 Å, thus indicative of a weak three-body chemical bond reminiscent of the nonclassical bond in metal dihydrides [18]. Compared to the other surface In, this In atom is lifted up toward the C-C pair by 0.3 Å. When forming the triangle, the nanotube also undergoes a slight radial deformation. In contrast, in the case of $(6, 0)/(\bar{1}\,\bar{1}\,\bar{1})$ where no such bond forms, neither indium displacement nor tube deformation is visible. One can qualitatively understand the above results in terms of a simple electronic model. The empty dangling-bond orbitals of the In atoms on the topmost (110) and (111) layers attract electrons in the doubly occupied C-C π orbitals of the nanotube. The attraction is, however, not strong enough to completely break the π bonds. As a result, only weak bonds form between In and C-C. On the other hand, the dangling-bond orbitals of the As atoms on the topmost $(\bar{1}\,\bar{1}\,\bar{1})$ layer are doubly occupied. This makes the formation of a bond between the surface As and C-C pair highly unlikely, because there is little energy incentive to form such a bond between two already doubly occupied orbitals.

Interacting nanotubes: IIa. Band structures (metal).—Figures 3(a)–3(c) project, for the metallic (6, 0) tube on different InAs surfaces, the wave functions to the following: (i) the nanotube (blue), (ii) the surface In atoms (green), and (iii) the surface As atoms (red). Any state residing in more than one region above can be expressed as a linear combination of the three prime colors: for example, a purple color in Fig. 3 would indicate a hybridized state between nanotube and surface As atoms. By comparing the projected states in Fig. 3 with those of isolated (6, 0) and InAs surfaces, we conclude that both the nanotube and surface maintain, to a large degree, their own electronic integrity, with minor changes reflected as level splitting due to symmetry lowering and radial deformation due to interfacial binding [6,7]. In addition, the surface potential is attractive to nanotubes within a bonding distance of about 3 Å. When compared with the band diagram in Fig. 2, only modest downward shifts of the (6, 0) tube band structure relative to those of

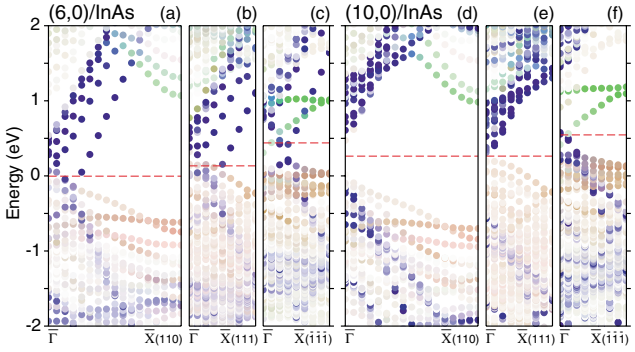

FIG. 3 (color). Site-decomposed band structures of a (6, 0) nanotube on (a) (110), (b) (111), and (c) $(\bar{1}\,\bar{1}\,\bar{1})$ surfaces of InAs in the direction of the tube axis. (d)–(f) Band structures of a (10, 0) nanotube. Colors indicate the predominant location of a state, being in the nanotube (blue), at the surface In sites (green), at the surface As sites (red), or their combination. Surface here is defined as the topmost monolayer, thus a single layer for (110) but a bilayer for both (111) and $(\bar{1}\,\bar{1}\,\bar{1})$. Horizontal red dashed lines indicate the Fermi level. The energy zero is set at the VBM of bulk InAs.

the surfaces are observed: 0.2 eV for (110) and 0.05 eV for both (111) and $(\bar{1}\,\bar{1}\,\bar{1})$.

Charge transfer between nanotubes and InAs surfaces may also result. For example, for a (6, 0) tube on the (110) surface [Fig. 3(a)], E_F is within the InAs band gap. Hence, there is little charge transfer. For a (6, 0) tube on the (111) surface [Fig. 3(b)], however, E_F is below the high-lying valence states of InAs, indicating that appreciable charge transfer may have taken place from surface to nanotube. For a (6, 0) tube on the $(\bar{1}\,\bar{1}\,\bar{1})$ surface [Fig. 3(c)], E_F is, instead, above the low-lying InAs surface states. Hence, charge transfer should also take place but in the reverse direction, i.e., from nanotube to surface.

Interacting nanotubes: IIb. Band structures (semiconductor).—Figures 3(d)–3(f) project the wave functions for the semiconducting (10, 0) tube on InAs(110), (111), and $(\bar{1}\,\bar{1}\,\bar{1})$ surfaces. Our basic observation for the metallic (6, 0) tube, e.g., the integrity of the tube and surface electronic states, appears to universally apply to the semiconducting (10, 0) tube. In addition, the (10, 0) tube on the nonpolar (110) surface has a similar band alignment to the (6, 0) tube, i.e., with a 0.2-eV downward shift relative to Fig. 2. For the polar surfaces, however, the shifts are much larger, -0.55 eV for (111) but $+0.57$ eV for $(\bar{1}\,\bar{1}\,\bar{1})$.

The reason for the large shifts is because of a relatively large surface dipole for the polar surfaces. The In-vacancy terminated (111)-2×2 surface exposes As dangling bonds (DBs) in the second surface layer. According to the electron-counting model [19], each In atom in the topmost layer donates 3/4 electrons to the As DB. This charge transfer results in a surface dipole pointing from the interior of the InAs to the surface. This causes a

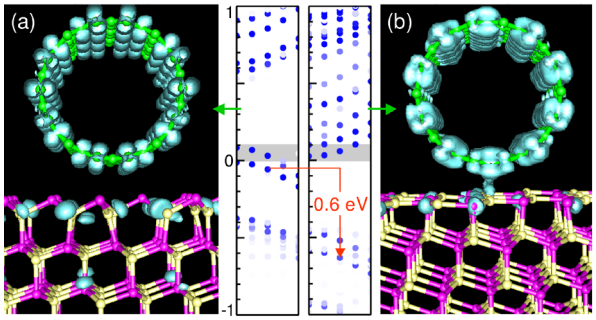

FIG. 4 (color online). Conducting channel charge densities for the p-type $(14, 0)$ on the $(\bar{1}\,\bar{1}\,\bar{1})$ surface (left) and the n-type $(14, 0)$ on the (111) surface (right). They are calculated by integrating from E_F to $E_F + 0.1$ eV [i.e., the shaded area in the middle panels in which projected tube band structures (excluding those of InAs surfaces) are shown]. Energy zero is the Fermi level, E_F, and the arrow indicates the shift of the overall tube states of 0.6 eV.

downward shift of the vacuum level relative to the interior of InAs. Accordingly, the tube electronic states are also downward shifted by the same amount. Conversely, the As-vacancy terminated $(\bar{1}\,\bar{1}\,\bar{1})$-$2 \times 2$ surface contains In DBs in the second layer. The charge transfer, thus, goes in the opposite direction. The resulting surface dipole points from the surface to the interior of the InAs. So both the vacuum level and the electronic states of the tube are upward shifted relative to the interior of InAs. Note that the surface dipole is a property of the surface itself. Thus, even for the nonbonding $(\bar{1}\,\bar{1}\,\bar{1})$ surface, significant shift can result. In contrast, there are no such large shifts for metallic $(6, 0)$ tube. The reason is because of the strong screening by the metallic states, which counteracts to minimize the dipole effect.

The above results show that carbon nanotubes behave more like extended molecules than solids. This suggests that the semiconductor surfaces may have the unexpected effect of doping the nanotubes either the n or the p type without, in the conventional sense, any actual dopants. In other words, this happens (i) when the tube CBM drops below the InAs VBM or (ii) when the tube VBM raises above the InAs CBM, namely, when a type-III band alignment between tube and InAs results, significant charge transfer must take place across the interface. We find that a $(14, 0)$ tube could, in fact, have both properties. Figure 4 shows the distribution of charge carriers from E_F to $E_F + 0.1$ eV for the p type $(14, 0)/(\bar{1}\,\bar{1}\,\bar{1})$ and the n type $(14, 0)/(111)$. It shows that most of the charge carriers remain on the nanotube. Only a small fraction is leaked to the semiconductor. It further shows that an overall 0.6 eV shift could result merely by changing the polarity of the surface from $(\bar{1}\,\bar{1}\,\bar{1})$ to (111). Autodoping a nanotube by different surface orientations without the actual dopants is a concept worthy of attention, not only because unintentional doping is often undesirable, but also because Coulomb scattering by charged dopants is often harmful. By removing the charged dopants, however, semiconducting nanotubes should also behave like *coherent* one-dimensional conductors.

In summary, our first-principles calculations laid the theoretical ground for nanotube wires on commensurate semiconductor surfaces. In the case of InAs, nanotubes preferentially bind to surface In atoms, while maintaining their own internal structural and electronic integrity. A universal band alignment is established for noninteracting tubes, which also holds approximately for interacting metallic tubes and for semiconducting tubes on nonpolar surfaces. On the other hand, the band structure of a semiconducting tube can be significantly shifted by polar surface dipole potentials. In the extreme cases, bipolar autodoping of the semiconducting nanotubes by different surface orientations is predicted. These findings may be important to the development of nanoscale hybrid electronic and optoelectronic devices formed using carbon nanotubes and conventional semiconductors.

We thank Yufeng Zhao for stimulating discussions. Y. H. K. and M. J. H. were supported by the U.S. Department of Energy, Office of Basic Energy Sciences, Division of Chemical Sciences, under Contract No. DE-AC36-99GO10337.

[1] N. Hamada *et al.*, Phys. Rev. Lett. **68**, 1579 (1992).
[2] S. M. Bachilo *et al.*, Science **298**, 2361 (2002).
[3] S. J. Tans *et al.*, Nature (London) **393**, 49 (1998); R. Martel *et al.*, Appl. Phys. Lett. **73**, 2447 (1998).
[4] A. Bachtold *et al.*, Science **294**, 1317 (2001); W. B. Choi *et al.*, Appl. Phys. Lett. **79**, 3696 (2001); R. Martel *et al.*, Phys. Rev. Lett. **87**, 256805 (2001); A. Javey *et al.*, Appl. Phys. Lett. **80**, 1064 (2002).
[5] J. A. Misewich *et al.*, Science **300**, 783 (2003).
[6] C.-J. Park *et al.*, Phys. Rev. B **60**, 10 656 (1999); J.-Q. Lu *et al.*, Phys. Rev. Lett. **90**, 156601 (2003).
[7] Y.-H. Kim and K. J. Chang, Phys. Rev. B **64**, 153404 (2001); J. O'Keefe *et al.*, Appl. Phys. Lett. **80**, 676 (2002).
[8] P. Hohenberg and W. Kohn, Phys. Rev. **136**, B864 (1964).
[9] D. M. Ceperley and B. J. Alder, Phys. Rev. Lett. **45**, 566 (1980).
[10] D. Vanderbilt, Phys. Rev. B **41**, 7892 (1990).
[11] G. Kresse *et al.*, http://cms.mpi.univie.ac.at/VASP.
[12] M. S. Dresselhaus *et al.*, *Science of Fullerenes and Carbon Nanotubes* (Academic Press, San Diego, 1996).
[13] W. Orellana *et al.*, Phys. Rev. Lett. **91**, 166802 (2003).
[14] The severe curvature of the $(6, 0)$ tube results in a lowering of the Fermi level with respect to that of graphene. X. Blase *et al.*, Phys. Rev. Lett. **72**, 1878 (1994).
[15] N. Moll *et al.*, Phys. Rev. B **54**, 8844 (1996).
[16] S.-H. Wei and A. Zunger, Appl. Phys. Lett. **72**, 2011 (1998).
[17] S. B. Zhang and A. Zunger, Phys. Rev. Lett. **77**, 119 (1996).
[18] G. J. Kubas, J. Organomet. Chem. **635**, 37 (2001).
[19] M. D. Pashley, Phys. Rev. B **40**, 10 481 (1989).